Strain-Specific Effects of Rosiglitazone on Bone Mass, Body Composition, and Serum Insulin-Like Growth Factor-I

Cheryl L. Ackert-Bicknell, Keith R. Shockley, Lindsay G. Horton, Beata Lecka-Czernik, Gary A. Churchill, and Clifford J. Rosen

The Jackson Laboratory (C.L.A.-B., K.R.S., L.G.H., G.A.C., C.J.R.), Bar Harbor, Maine 04609; and Department of Orthopaedic Surgery and Physiology (B.L.-C.), University of Toledo Medical Center, Toledo, Ohio 43614

Activation of peroxisome proliferator activated receptor-γ (PPARG) is required for the differentiation of marrow mesenchymal stem cell into adipocytes and is associated with the development of age-related marrow adiposity in mice. Thiazolidinediones are agonists for PPARG and have a heterogeneous effect on bone mineral density (BMD). We postulated that genetic determinants influence the skeletal response to thiazolidinediones. We examined the effects of rosiglitazone (3 mg/kg · d for 8 wk) on BMD, body composition, and serum IGF-I in adult female mice from four inbred strains. C3H/HeJ mice showed the most significant response to treatment, exhibiting decreased femoral and vertebral BMD, reduced distal femoral bone volume fraction and a decrease in serum IGF-I. In DBA/2J, there were no changes in femoral BMD or bone volume fraction, but there was a decrease in vertebral BMD. C57BL/6J mice showed increases in marrow adiposity, without associated changes in trabecular bone volume; the skeletal effects from rosiglitazone in A/J mice were minimal. No association between trabecular bone volume and marrow adiposity was found. The effect of rosiglitazone on gene expression in the femur was then examined in the C3H/HeJ and C57BL/6J strains by microarray. Increased gene expression was observed in the PPARG signaling pathway and fatty acid metabolism in both C3H/HeJ and C57BL/6J, but a significant down-regulation of genes associated with cell cycle was noted only in the C3H/HeJ strain. The divergent skeletal responses to rosiglitazone in this study suggest the existence of a strong genetic background effect. (***Endocrinology*** **150: 1330–1340, 2009)**

Thiazolidinediones (TZDs) are a class of chemical compounds that are selective agonists of the nuclear receptor peroxisome proliferator-activated receptor-γ (PPARG) (1). TZDs are insulin-sensitizing agents and two members of this chemical class, rosiglitazone and pioglitazone, are widely prescribed for the treatment of type II diabetes (2). Rosiglitazone has also been investigated as a potential preventative agent in patients at high risk of developing type 2 diabetes (3). Troglitazone was available from the late 1990s until early 2000 for the treatment of type II diabetes, but this drug was withdrawn from clinical use due to liver complications (2).

PPARG belongs to a family of nuclear receptors and transcription factors. The PPARG proteins form heterodimers with the retinoic acid receptor-α, and in the presence of specific ligands, this heterodimer is able to induce gene transcription. Naturally occurring ligands for PPARG include polyunsaturated fatty acids and metabolic derivatives of prostaglandins (reviewed in Ref. 4). Expression of *Pparg* is required for the maturation of adipocytes (*5*), but the expression networks that both control *Pparg* expression and are controlled by activated PPARG protein have not been fully resolved. During adipogenesis CCAAT/enhancer-binding protein-β (*Cebpb*) has been shown to induce the expression of *Pparg* and in turn, PPARG can then induce the expression of CCAAT/enhancer-binding protein-α (*Cebpa*) (6). In bone, marrow mesenchymal stem cells (MSCs) are able to give rise to a variety of terminally differentiated cell types, including osteoblasts, chondrocytes, and adipocytes. Activation of PPARG is required for the differentiation of these MSCs into adipocytes

ISSN Print 0013-7227 ISSN Online 1945-7170
Printed in U.S.A.

doi: 10.1210/en.2008-0936 Received June 24, 2008. Accepted October 16, 2008.
First Published Online October 23, 2008

Abbreviations: aBMD, Areal BMD; BMD, bone mineral density; BV, volume of the trabecular bone; BV/TV%, trabecular bone volume fraction; μCT, microcomputed tomography; KEGG, Kyoto Encyclopedia of Genes and Genomes; MSC, mesenchymal stem cell; PPARG, peroxisome proliferator-activated receptor-γ; pQCT, peripheral quantitative computed tomography; SNP, single-nucleotide polymorphism; TV, volume of the distal femoral marrow cavity; TZD, thiazolidinedione; vBMD, volumetric BMD.

(1, 7, 8). Studies in humans have shown that the degree of marrow adiposity increases with age and that the extent of marrow adiposity is inversely correlated to levels of bone formation (9–14). These observations in humans, together with animal studies, have led to the hypothesis that any increase in marrow adiposity will have negative consequences for bone (15).

Studies in C57BL/6J male mice have shown that treatment with high doses of rosiglitazone (20 mg/kg · d) results in bone loss and increased marrow adiposity in both adult and old mice but not in young growing animals (16). In Swiss-Webster mice treated with rosiglitazone, bone loss was observed, but this was in young adult animals (17). In respect to human studies, in the Dynamics of Health, Aging and Body Composition (Health ABC) cohort, Schwartz *et al.* reported that TZD treatment was associated with a decrease in BMD in women but not men (18), whereas in an unrelated study population, Yaturu *et al.* (19) reported a decrease in bone mineral density (BMD) in men treated with rosiglitazone. In contrast, Watanabe *et al.* (20) reported that treatment with troglitazone was associated with an increase in BMD in some but not all patients. In addition, no change in percent body fat was found in treated patients. Whereas this study included both men and women, response to treatment was not partitioned by gender (20).

Peak bone mass is inherited in a polygenic fashion, and studies suggest that between 55 and 80% of the variance in peak bone mass is attributable to heritable factors (reviewed in Ref. 21). Environmental factors such as diet and exercise also contribute to peak bone mass. The Health ABC cohort is composed of both whites and blacks (18), whereas all patients in the cohort studied by Watanabe *et al.* (20) were Japanese. In the study by Yaturu *et al.* (19), only men were examined and no description of the ethnic composition of the study cohort was provided. The conflicting results in these two ethnically divergent populations suggest that the effect of TZDs on bone is influenced by heritable factors. In this study, we hypothesized that skeletal responses to rosiglitazone are determined by genetic background. The effect of a low dose of rosiglitazone (3 mg/kg · d) on bone was investigated in female mice from four inbred strains of mice. Each of the strains exhibited a different response to rosiglitazone treatment with regards to bone mass, body composition measures, and serum IGF-I.

Materials and Methods

Animals and diets

All studies and procedures were approved by the Institutional Animal Care and Use Committee of the Jackson Laboratory. All mice used in these experiments were female. The A/J (stock no. 000646) and DBA/2J (DBA, stock no. 000671) mice were purchased from the resource colonies of The Jackson Laboratory. The C57BL/6JBm (B6) and C3H/HeJ (C3H) mice were obtained from our research colony. Mice had free access to water and diet for the duration of the study.

For studies examining the effect of rosiglitazone on bone, body composition, and serum IGF-I, groups of 10–14 young adult mice of each strain were placed on either control diet or a diet supplemented with rosiglitazone. Mice were 16 wk of age at the start of the experiment and were maintained on dietary treatment until they were 26 wk of age. Body weights, body composition, and whole-body areal BMD (aBMD) data were collected at the conclusion of the experiment. Femurs were also collected and fixed in 95% ethanol for subsequent volumetric BMD (vBMD), microcomputed tomography (μCT) analyses, and histological analyzes.

The control diet was 5K52 from LabDiet (St. Louis, MO). This is an NIH31, 6% fat (by weight), diet and is a standard rodent diet used at The Jackson Laboratory. To assess the affects of rosiglitazone, the control diet was supplemented with rosiglitazone (0.02 mg per 1 g of diet). This diet composition was chosen such that each mouse would ingest a dose of 3 mg of rosiglitazone per 1 kg of body weight per day (3 mg/kg · d), based on previous food consumption experiments by both ourselves and others (http://phenome.jax.org/pub-cgi/phenome/mpdcgi?rtn=docs/home).

A similar protocol was followed for gene expression studies. In this experiment, groups of five B6 and 5 C3H mice were placed on either a control diet or a diet supplemented with rosiglitazone as described above. Mice were placed on diet at 8 wk of age and maintained on diet for 8 weeks.

Dual-energy x-ray absorptiometry

aBMD and body composition were assessed using peripheral dual-energy x-ray absorptiometry (PIXImus; GE-Lunar, Madison, WI). The scans assessed whole-body (exclusive of the head) bone mineral content and aBMD as well as whole-body lean mass, fat mass, and percent body fat. The short-term coefficient of variation for repeat measures of total body aBMD was 8.3%.

Peripheral quantitative computed tomography (pQCT)

Femur lengths were measured with digital calipers (Stoelting, Wood Dale, IL), and then femurs were measured for density using the SA Plus densitometer (Orthometrics; Stratec SA Plus Research Unit, White Plains, NY). Calibration of the SA Plus instrument was established with hydroxyapatite standards of known density (50–1000 mg/mm^3) with cylindrical diameters 2.4 mm and length 24 mm that approximates mouse femurs. Daily quality control of the SA Plus instrument's operation was checked with a manufacturer-supplied phantom. The bone scans were analyzed with threshold settings to separate bone from soft tissue. Thresholds of 710 and 570 mg/cm^3 were used to determine cortical bone areas and surfaces that yielded area values consistent with histomorphometrically derived values. To determine mineral content, a second analysis was carried out with thresholds of 220 and 400 mg/cm^3 selected so that mineral from most partial voxels (0.07 mm) were included in the analysis. Density values were calculated from the summed areas and associated mineral contents. Precision of the SA Plus for repeated measurement of a single femur was found to be 1.2–1.4%. Isolated femurs were scanned at seven locations at 2-mm intervals, beginning 0.8 mm from the distal ends of the epiphyseal condyles. Total vBMD values were calculated by dividing the total mineral content by the total bone volume and expressed as milligrams per cubic millimeter. Periosteal circumference and cortical thickness measures were made at the exact midshaft of the femur.

μCT

Femurs were scanned using a Micro CT40 microcomputed tomographic instrument (Scanco Medical AG, Bassersdorf, Switzerland) to evaluate trabecular bone volume fraction and microarchitecture in the secondary spongiosa of the distal femur. Daily quality control of the instrument's operation was checked with a manufacturer-supplied phantom. The femurs were scanned at low-resolution energy level of 55 KeV and intensity of 145 μA. Approximately 100 slices were measured just proximal to the distal growth plate, with an isotropic pixel size of 12 μm and slice thickness of 12 μm. Trabecular bone volume fraction (BV/TV%) and microarchitecture properties of trabecular number, thickness, and spacing were evaluated in the secondary spongiosa, starting approximately 0.6 mm proximal to the growth plate and extending proximally 1.5 mm.

Histology

Five bones per treatment group were analyzed for marrow adiposity. Bones were fixed in 95% ethanol for a minimum of 2 wk. The musculature was removed and bones were further fixed in ethanol for a minimum of 3 wk. Bones were decalcified for 24 h in Cal-EX (no. CS510-1D;

TABLE 1. Body composition

Strain	Treatment	Body weight (g)		Fat (g)[a,b]		Lean (g)[a,b]	
		Average	*P* value	Average	*P* value	Average	*P* value
B6	Control	21.67 ± 0.76	0.208	4.61 ± 0.20	0.025	16.34 ± 0.20	0.102
	Rosi	22.96 ± 0.64		5.27 ± 0.17		15.9 ± 0.16	
C3H	Control	23.32 ± 0.75	0.160	5.13 ± 0.44	0.789	17.16 ± 0.34	0.584
	Rosi	24.93 ± 0.82		5.31 ± 0.48		17.47 ± 0.37	
DBA	Control	25.82 ± 1.01	0.980	7.31 ± 0.20	0.181	18.19 ± 0.22	0.051
	Rosi	25.86 ± 1.01		7.70 ± 0.20		17.54 ± 0.22	
A/J	Control	23.22 ± 0.60	0.623	5.92 ± 0.16	0.009	16.53 ± 0.14	0.030
	Rosi	23.65 ± 0.60		6.57 ± 0.16		16.07 ± 0.14	
Strain × Rosi		0.7293		0.3932		0.0484	

Rosi, Rosiglitazone.

[a] Body weight was a significant covariate for all strains.

[b] The interaction factor of body weight × treatment was a significant covariate for DBA/2J only.

Fisher Scientific, Pittsburgh, PA) and rinsed in tap water for 72 h. Femurs were embedded in paraffin and serial sectioned along the sagittal plane at a thickness of 5 μm until sections of the center of the distal femur were obtained. Sections were stained with hematoxylin and eosin using standard methodologies, and sections were viewed with a DMRXE upright light microscope (Leica, Wetzlar, Germany). One field per femur was photographed with a Leica DFC300FX color charge-coupled device camera from the center of the bone immediately proximal to the growth plate. The number of adipocytes per field were counted. Because these tissues had been dehydrated in ethanol, lipid content had also been extracted. Adipocytes appear as oval holes in the sections that are devoid of staining.

Serum IGF-I

Serum IGF-I was measured by RIA (ALPCO, Windham, NH) as previously described (22). IGF binding proteins were first removed from the IGF-I by an acid dissociation step. This was followed by the addition of a neutralization buffer containing excess recombinant human IGF-II, allowing the IGF-II to bind to the IGF binding proteins before immunoassay with a human anti-IGF-I polyclonal antibody. The sensitivity of the assay was 0.01 ng/ml IGF-I; the interassay coefficient of variation based on normal standards and pooled serum of C^3H and B6 was approximately 6%. There is no cross-reactivity with IGF-II. Standards were run in each assay as well as normal pools from both B6 and C3H mice.

Serum osteocalcin

Serum osteocalcin was measured by immunoradiometric assay as per the manufacturer's instructions (ALPCO). The interassay coefficient of variation based on normal standards and pooled serum from B6 mice was approximately 2.3%. Manufacturer-provided standards were run in each assay as well as normal serum pools from B6 mice.

Statistics

Data are expressed as mean ± SEM in tables and figures. Statistical evaluation of bone and body composition was conducted using JMP version 6 software (SAS, Cary, NC). To account for differences in body size between strains, a stepwise analysis of covariance approach was used for pQCT and μCT data using body weight and femur length as covariates. Nonsignificant covariates and interactions were removed in a stepwise fashion until the final model remained. The effect of treatment was first examined in each strain independent of all other strains and differences between control and treatment was determined by Student's *t* test. In a second analysis, the effect strain, treatment, and strain by treatment were examined. The F-statistic for the interaction factor is presented.

Genetic comparisons between strains

Single-nucleotide polymorphism (SNP) differences within the *Pparg* gene were examined using publicly available resources found on the Mouse Phenome Database (http://www.jax.org/phenome/snp.html). More specifically, analysis was accomplished using the Mouse Phenome Database SNP Tools resource package. Differences in the *Pparg* gene were examined using graphical SNP strain comparison tool.

TABLE 2. vBMD

Strain	Treatment	Total femoral vBMD (mg/mm^3)[a]		Femoral cortical vBMD (mg/mm^3)		Total L5 vBMD (mg/mm^3)[b]	
		Average	*P* value	Average	*P* value	Average	*P* value
B6	Control	0.609 ± 0.008	0.108	1.117 ± 0.008	0.213	0.290 ± 0.006	0.027
	Rosi	0.593 ± 0.006		1.104 ± 0.006		0.272 ± 0.005	
C3H	Control	0.947 ± 0.007	<0.0001	1.283 ± 0.004	0.015	0.319 ± 0.008	0.040
	Rosi	0.869 ± 0.008		1.267 ± 0.004		0.292 ± 0.009	
DBA	Control	0.693 ± 0.007	0.083	1.212 ± 0.005	0.954	0.282 ± 0.006	0.0009
	Rosi	0.675 ± 0.005		1.211 ± 0.005		0.246 ± 0.006	
A/J	Control	0.678 ± 0.009	0.705	1.195 ± 0.004	0.012	0.268 ± 0.011	0.449
	Rosi	0.683 ± 0.009		1.180 ± 0.004		0.280 ± 0.011	
Strain × Rosi		<0.0001		0.5493		0.0014	

Rosi, Rosiglitazone.

[a] Body weight was a significant covariate for A/J only.

[b] Body weight was a significant covariate for C57BL/6J and C^3H/HeJ.

TABLE 3. Whole-body aBMD (g/cm^2)

Strain	Treatment	Average	*P* value
B6	Control	0.0504 ± 0.0005	0.007
	Rosi	0.0484 ± 0.0004	
C3H	Control	0.0608 ± 0.0004	0.005
	Rosi	0.0591 ± 0.0004	
DBA	Control	0.0510 ± 0.0004	0.159
	Rosi	0.0501 ± 0.0004	
A/J	Control	0.0466 ± 0.0005	0.659
	Rosi	0.0469 ± 0.0005	
Strain × Rosi		0.0176	

Body weight was a significant covariate for DBA/2J and A/J. Rosi, Rosiglitazone.

Gene expression

Bone samples were stored frozen after dissection. For the RNA extraction, the bones were first pulverized and then homogenized in TRIzol (Invitrogen, Carlsbad, CA). Total RNA was isolated by standard TRIzol methods according to the manufacturer's protocols, and quality was assessed using an Agilent 2100 bioanalyzer instrument and RNA 6000 Nano LabChip assay (Agilent Technologies, Palo Alto, CA). Total RNA was then reverse transcribed followed by second-strand cDNA synthesis. An *in vitro* transcription reaction was carried out incorporating biotinylated nucleotides according to the manufacturer's protocol for Illumina Totalprep RNA amplification kit (Ambion, Austin TX). Then 1.5 μg biotin-labeled cRNA was hybridized onto Mouse-6 Expression BeadChip (Illumina, San Diego CA) for 16 h at 55 C. Posthybridization staining and washing were performed according to the manufacturer's protocols (Illumina). BeadChips were then scanned using Illumina's BeadStation 500 scanner. Images are checked for grid alignment and then quantified using the BeadStudio software. A first-pass read of the control summary graphs generated by BeadStudio is the quality control for hybridization, washing stringency, and background.

Summarized data from BeadChip Mouse Sentrix-6 arrays was read into the R software environment. Data quality was assessed using histograms of raw signal intensities and MvA plots. Normalization was carried out using quantile normalization (23) to form one expression measure per gene per array. Log-transformed expression measures were expressed in fixed-effects ANOVA models as the sum of different components contributing to the overall intensity value of each gene on the array. First, the model, $Y_i = \mu + \text{group} + \varepsilon_i$ (equation 1), was fit to the log-transformed gene expression measures Y_i, where μ is the mean for each array, group is the effect for each experimental group, and ε_i captures random error. A modified F-statistic that assesses differential expression between experimental groups was used as a statistical filter to select one probe set for each mapped Entrez gene on the array when appropriate (24).

To test for differences due to rosiglitazone, the data were subset by strain (*i.e.* B6 and C3H) and a model was fit ($Y_i = \mu + \text{drug} + \varepsilon_i$) (equation 2) where drug refers to the presence or absence of rosiglitazone in the diet. All statistical tests were conducted with F-statistic, a modified F-statistic incorporating shrinkage variance components that allows variance estimates to include information from all the probe sets on the array (24). Critical *P* values were calculated by permuting model residuals 1000 times and pooling F-statistics (25). False-discovery rate values were estimated for each test result by implementing the q-value method of Storey (26).

Kyoto Encyclopedia of Genes and Genomes (KEGG) pathway analysis

Pathways from KEGG enriched for genes whose expression was altered due to rosiglitazone were identified using a random-set enrichment scoring method (27). First, an F-statistic corresponding to differences due to diet in equation 2 was calculated for each probe in the data set. Square-root transformed F-statistic values were assigned to be positive for probes with higher average expression in the presence of rosiglitazone and given negative values for probes with higher average expression without rosiglitazone in the diet. Standardized enrichment scores (Z scores) have a mean zero and unit variance score on the null hypothesis that the pathway is not enriched for differentially expressed genes. The Z scores computed for each KEGG pathway were adjusted for overrepresentation of genes in the system using the adjustment method of (27).

Results

Body composition

The effect of treatment with rosiglitazone with regard to changes in body composition was unique in each strain (Table 1). None of the strains displayed a significant difference in body weight when comparing the treated *vs.* the untreated animals. Interestingly, the A/J strain showed a significant increase in body fat along with a decrease in lean mass, resulting in no net change in body weight. The B6 mice showed a significant increase in body fat, which was not associated with a change in body weight. Neither the C3H nor the DBA strains showed statistically significant changes in body weight or body composition with rosiglitazone treatment. The F-statistic for the interaction effect

TABLE 4. Femur size

		Length (mm)[a]		Cortical thickness (mm)[b]		Periosteal circumference (mm)[a]	
Strain	Treatment	Average	*P* value	Average	*P* value	Average	*P* value
B6	Control	15.55 ± 0.09	0.062	0.200 ± 0.003	0.185	5.07 ± 0.03	0.002
	Rosi	15.32 ± 0.07		0.194 ± 0.003		4.93 ± 0.02	
C3H	Control	15.75 ± 0.07	0.040	0.393 ± 0.008	0.013	4.77 ± 0.05	0.681
	Rosi	15.52 ± 0.08		0.363 ± 0.008		4.74 ± 0.05	
DBA	Control	15.16 ± 0.08	0.265	0.243 ± 0.005	0.983	4.16 ± 0.04	0.841
	Rosi	15.29 ± 0.08		0.243 ± 0.004		4.17 ± 0.03	
A/J	Control	15.28 ± 0.08	0.517	0.224 ± 0.007	0.296	4.28 ± 0.04	0.785
	Rosi	15.20 ± 0.08		0.213 ± 0.007		4.26 ± 0.04	
Strain × Rosi		0.0331		0.0339		0.8553	

Rosi, Rosiglitazone.

[a] Body weight was a significant covariate for B6 only.

[b] Body weight was a significant covariate for A/J only.

TABLE 5. Distal femoral trabecular volume fraction

Strain	Treatment	BV (mm^3)[a]		TV (mm^3)[b]		BV/TV (%)[c]	
		Average	*P* value	Average	*P* value	Average	*P value*
B6	Control	0.149 ± 0.009	0.794	2.03 ± 0.06	0.789	6.6 ± 0.4	0.170
	Rosi	0.153 ± 0.008		2.05 ± 0.05		7.4 ± 0.3	
C3H	Control	0.641 ± 0.024	0.075	1.45 ± 0.04	0.004	44.2 ± 1.6	0.001
	Rosi	0.573 ± 0.027		1.65 ± 0.04		35.1 ± 1.7	
DBA	Control	0.085 ± 0.007	0.279	1.57 ± 0.02	0.001	5.3 ± 0.4	0.649
	Rosi	0.097 ± 0.007		1.72 ± 0.02		5.6 ± 0.4	
A/J	Control	0.175 ± 0.023	0.834	1.72 ± 0.03	0.010	10.3 ± 1.1	0.361
	Rosi	0.167 ± 0.023		1.85 ± 0.03		8.8 ± 1.1	
Strain × Rosi		0.2547		0.0255		< 0.0001	

Rosi, Rosiglitazone.

[a] Femur length was a significant covariate for DBA/2J only.

[b] Body weight was a significant covariate for C3H/HeJ and DBA/2J. Femur length was also a significant covariate for C^3H/HeJ.

[c] Body weight was a significant covariate for C57BL/6J and A/J. The interaction term of body weight × treatment was also a significant covariate for C57BL/6J. Femur length was a significant covariate for DBA/2J only.

strain × rosiglitazone treatment is presented at the bottom of Table 1.

BMD

The vBMD of the femur and L5 vertebrae was assessed by pQCT (Table 2), whereas the aBMD for the whole skeleton, exclusive of the skull, was assessed by dual-energy x-ray absorptiometry (Table 3). The statistically significant covariates for each measure of BMD are showed at the bottom of each table and the F-statistic for the interaction effect strain × rosiglitazone treatment is presented at the bottom of each column. The strain most affected by rosiglitazone, with regard to bone density, was C3H. Mice of this strain treated with rosiglitazone exhibited lower BMD at all sites measured *vs*. controls. In the A/J strain, no changes in total femoral and vertebral vBMD nor whole-body aBMD were noted, but a significant decrease in the cortical component the femur was found. The interaction effect of strain × rosiglitazone treatment was not significant for cortical vBMD. The effects of rosiglitazone treatment for the remaining two strains was much more site specific, with the vertebrae being more susceptible to treatment than the femur. For the B6 strain, treated animals had decreased whole-body aBMD and lower vertebral vBMD, but changes in the femur between rosiglitazone and controls were not statistically significant. Neither whole-body aBMD nor cortical bone density of the femur changed in response to rosiglitazone in the DBA/2J strain. Total vBMD of the femur was slightly lower in treated DBA/2J mice, whereas vertebral vBMD was markedly decreased in the treated mice.

Femur size

The femurs of rosiglitazone-treated C3H mice were significantly shorter than age-matched control-treated mice (Table 3). Rosiglitazone-treated B6 mice also tended to have shorter femurs, but this result was not statistically significant. No effect was seen for femur length in either the A/J or DBA strain. The midshaft cortical thickness and midshaft periosteal circumference data, presented Table 4, were obtained by pQCT. In the C3H strain, a decrease in cortical thickness was noted, but no change in periosteal circumference was observed. In the B6 strain, the periosteal circumference was found to be smaller, but this was not accompanied by changes in cortical thickness. No changes in these two measures were found in either the DBA or A/J strains. The F-statistic for the interaction effect strain × ros-

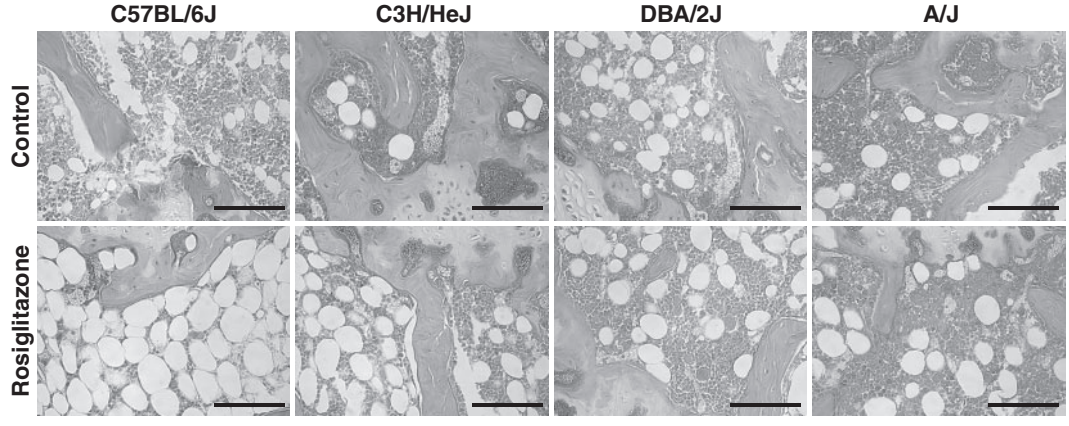

FIG. 1. μCT images of the distal femur. Digital reconstructions of the trabecular architecture of the distal femur are presented from the four inbred strains examined. Images from the control-treated mice are present in the *top row* and images from the rosiglitazone-treated mice are present in the *bottom row*. It is interesting to note that all strains except B6 exhibited an increase in TV. Only the C3H strain showed a significant change in the trabecular BV and the BV/TV%.

TABLE 6. Marrow adiposity

Strain	Treatment	Adipocytes (n) Average	*P* value
B6	Control	31.0 ± 4.8	0.006
	Rosi	72.3 ± 8.3	
C3H	Control	17.8 ± 7.2	0.063
	Rosi	36.8 ± 5.0	
DBA	Control	30.6 ± 9.9	0.295
	Rosi	44.4 ± 7.3	
A/J	Control	14.0 ± 4.6	0.226
	Rosi	22.6 ± 4.7	

Rosi, Rosiglitazone.

iglitazone treatment is presented at the bottom of each column of Table 4.

Trabecular volume fraction and marrow adiposity

The architecture of the trabecular bone was assessed in the distal femur by μCT and is shown in Table 5. Treatment with rosiglitazone resulted in an increase in the total volume of the distal femoral marrow cavity (TV) in all strains, except B6. In the C3H strain, the volume of the trabecular bone (BV) in this same location was decreased resulting in an overall reduction in BV/TV%. The number of trabeculae was significantly decreased in rosiglitazone-treated B6 ($P = 0.0284$) and C3H mice ($P = 0.0004$) as is shown in Fig. 1. Connectivity density, a measure of bone quality (28), was also found to be decreased in both the B6 ($P = 0.038$) and the C3H strains ($P = 0.003$). No change for this measure was noted in either A/J ($P = 0.225$) or DBA/2J ($P = 0.355$, data not shown). Marrow adiposity of distal femur was substantially higher in the B6 and moderately increased in the C3H mice-treated with rosiglitazone, compared with the control-treated mice (Table 6 and Fig. 2).

Serum measures

At the start of the experiment, the serum IGF-I levels were not different between the control groups and the groups-treated with rosiglitazone (data not shown). After 1 wk of treatment, as shown in Fig. 3A, serum IGF-I was significantly lower in the rosiglitazone-treated group for the B6 and the C3H strains. At the end of the experiment, the rosiglitazone-treated groups exhibited lower serum IGF-I than the control group for the B6, C3H, and A/J strains (Fig. 3B) but not DBA. The interaction effect of strain × rosiglitazone treatment was significant for at both 1 wk of treatment (F-statistic = 0.05) and at the conclusion of the experiment (F-statistic < 0.0001).

Osteocalcin, a marker of bone formation, was found to be significantly decreased in the treated A/J animals yet was found to be greatly increased in the treated DBA/2J mice (Fig. 4). No change in this serum marker was noted for the other two strains. The effect strain × rosiglitazone treatment was found to be significant (F-statistic < 0.0001).

Genetic comparisons between strains

The C3H strain displayed the greatest response to rosiglitazone. If we compare allelic differences in SNPs in C3H compared with B6, A/J, and DBA/2J combined (Fig. 5A), there are many regions across the genome in which this strain is quite different from the other strains. One such region is the location of the *Pparg* gene on chromosome 6, which is highlighted in blue (Fig. 5A). The genomic interval containing the *Pparg* gene was then examined for primary haplotype differences in a pairwise manner with the strains used in this study and using B6 as the base strain for comparison (*i.e.* B6 *vs.* DBA, B6 *vs.* A/J, B6 *vs.* C3H). B6 and C3H carry very different haplotypes for the *Pparg* gene (Fig. 5B), but B6 shares the same haplotype as A/J (Fig. 5C) and DBA/2J (Fig. 5D).

Gene expression

Gene expression in the femur was examined by microarray, comparing the effect of rosiglitazone in the B6 and the C3H strains. Our analyses were designed to identify the molecular pathways in which rosiglitazone altered gene expression in a differential manner when comparing the B6 with the C3H strain. These results are summarized in Table 7. A negative Z-score

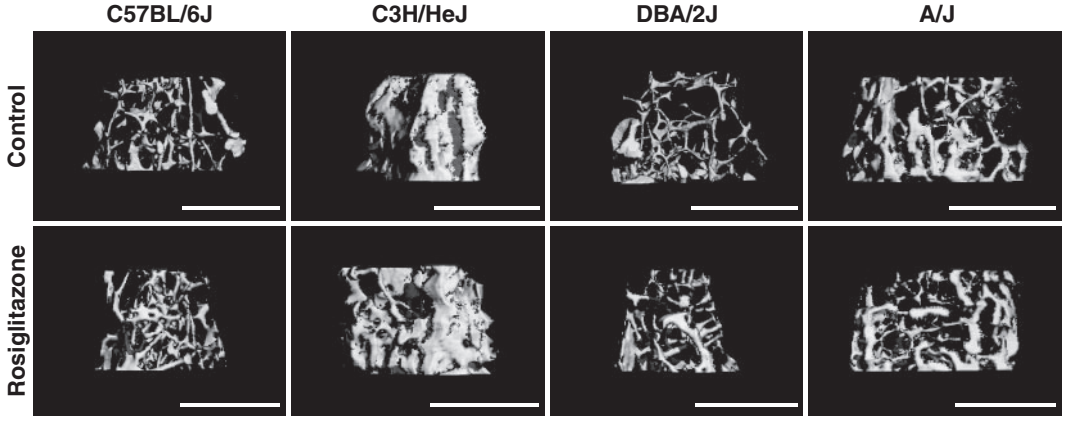

FIG. 2. Static histology of the distal femoral marrow cavity. All images display in the center of the marrow cavity immediately proximal to the growth plate. Samples were decalcified, embedded in paraffin, sectioned, and then stained with hematoxylin and eosin. Images from the control-treated mice are present in the *top row* and images from the rosiglitazone-treated mice are present in the *bottom row*. As can be seen, there is little difference in the number of marrow adipocytes when comparing the control-treated samples. Rosiglitazone treatment resulted in a substantial increase in marrow adiposity in the B6 mice and slight increase in the C3H mice. Interestingly, in B6-treated mice, red marrow has been nearly replaced by adipocytes, but BV/TV% was not affected by rosiglitazone treatment. No changes were observed in the DBA or A/J mice.

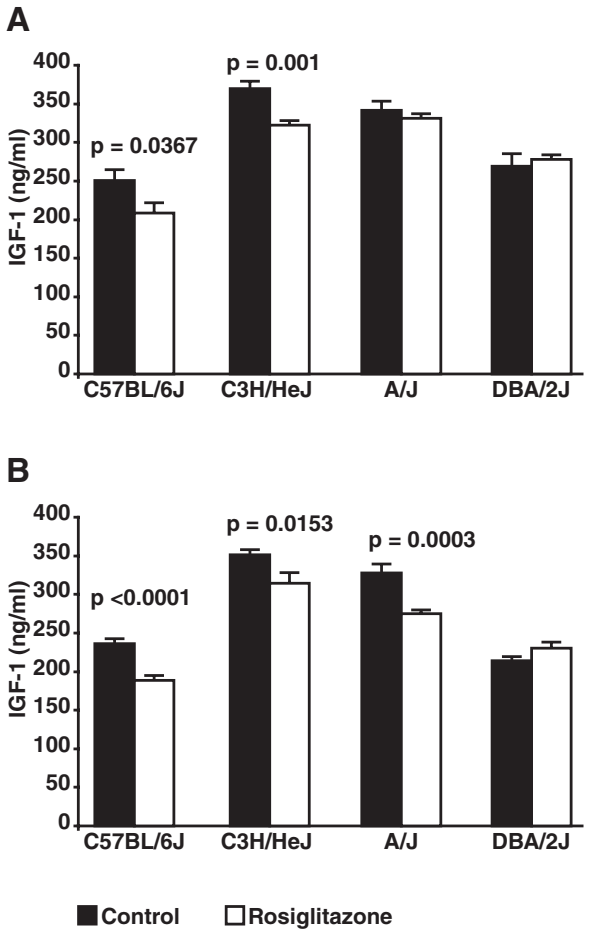

FIG. 3. Serum IGF-I. Serum IGF-I was assessed at baseline, after 1 wk of treatment, and at the conclusion of the experiment. A, The serum IGF-I levels in the B6 and C3H mice treated with rosiglitazone were significantly lower after 1 wk of treatment, compared with the controls. There was no difference found in the DBA and A/J strains. B, A similar difference in serum IGF-I was noted at the conclusion of the experiment for B6 and C3H. Unlike at 1 wk of treatment, serum IGF-I levels were decreased in the A/J strain after 8 wk of rosiglitazone treatment.

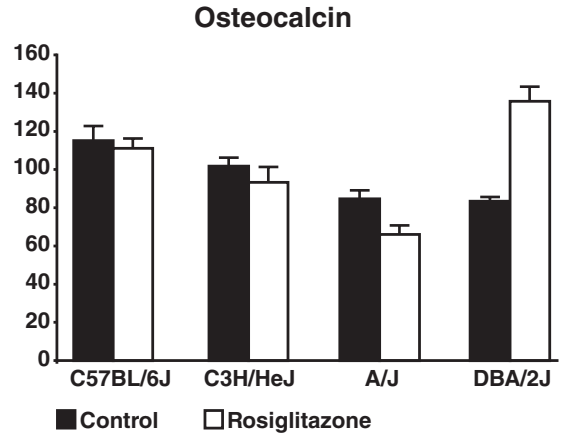

FIG. 4. Serum osteocalcin. Serum osteocalcin was measured in all mice at the conclusion of treatment. After 8 wk of treatment, note differences in serum osteocalcin were found for either the B6 or C3H strain. A significant decrease was noted in the A/J strain and a significant increase was noted for the DBA/2J strain.

indicates, that for that strain, rosiglitazone was associated with decreased gene expression for genes found in that pathway. A positive Z-score indicates increased expression. As expected, in both strains we observed an increase in expression in genes involved in the PPAR signaling, but this up-regulation of PPAR signaling was not significantly different between the two strains. The most significant effect observed was on genes known to be involved with cell cycle. A significant suppression of cell cycle genes was observed in the C3H strain, whereas there was no significant effect on cell cycle in B6. A similar pattern was observed for pyrimidine metabolism and ubiqutin mediated proteolysis. In contrast, an increase in nitrogen metabolism was noted on treatment in B6, whereas drug treatment had no effect in C3H.

Discussion

Four common strains of inbred mice were used in this study: C57BL/6J, C3H/HeJ, DBA/2J, and A/J. A recent study examining the phylogenetic relationship among inbred strains demonstrated that these four strains are genetically distinct from each other (29). Each of these strains exhibited a unique and strain-specific response to treatment with low-dose rosiglitazone in respect to skeletal parameters, body composition, and serum IGF-I. The C3H strain, in particular, demonstrated an extremely deleterious skeletal response to this drug. These results suggest the existence of a genotype by drug interaction for the TZDs relative to body composition and bone mass.

The C3H strain has been shown to have high vBMD that is coincident with high serum IGF-I levels, but these mice have similar body weight and femur length compared with B6 mice (30–32). Whereas no differences in body composition were seen with TZD treatment in C3H, all measures of BMD were decreased, despite the high baseline BMD. Also, C3H was the only strain to exhibit a net loss of BV/TV%. Interestingly, C3H, like B6 showed an increase in marrow adiposity of the distal femur in response to rosiglitazone. Like the B6 strain, serum IGF-I levels decreased in C3H with only 1 wk of rosiglitazone treatment and remained decreased at the conclusion of the experiment.

In mice, the epiphyses do not close and as a result, longitudinal bone growth continues, albeit at a slower rate by 4 months of age (30). In this study, treatment was initiated at 4 months of age, yet the effect on femur length was quite significant in the C3H mice; a similar trend was noted for DBA/2J. Previous examination of femur lengths in inbred strains has shown that the rate of growth of the femur in C3H is normally comparable with other inbred strains of mice, including B6 and DBA/2J (30). Wang *et al.* (33) have shown that activation of PPARG by TZDs inhibits differentiation of isolated chondrocytes. Our results are consistent with the studies of Wang *et al.* and suggest that rosiglitazone may alter femoral growth rate in a strain-specific manner.

The other three strains (B6, DBA, and A/J) showed varying degrees of phenotypic change in response to rosiglitazone. A/J skeleton was resistant to rosiglitazone, but this strain showed significant increases in percent body fat and decreases in serum osteocalcin. These observations are particularly intriguing for two reasons. First, of the four strains studied, C3H and A/J are the most closely related phylogenetically. Yet the skeletal and metabolic responses were quite distinct (29). Second, the changes in serum osteocalcin after treatment with rosiglitazone by strain

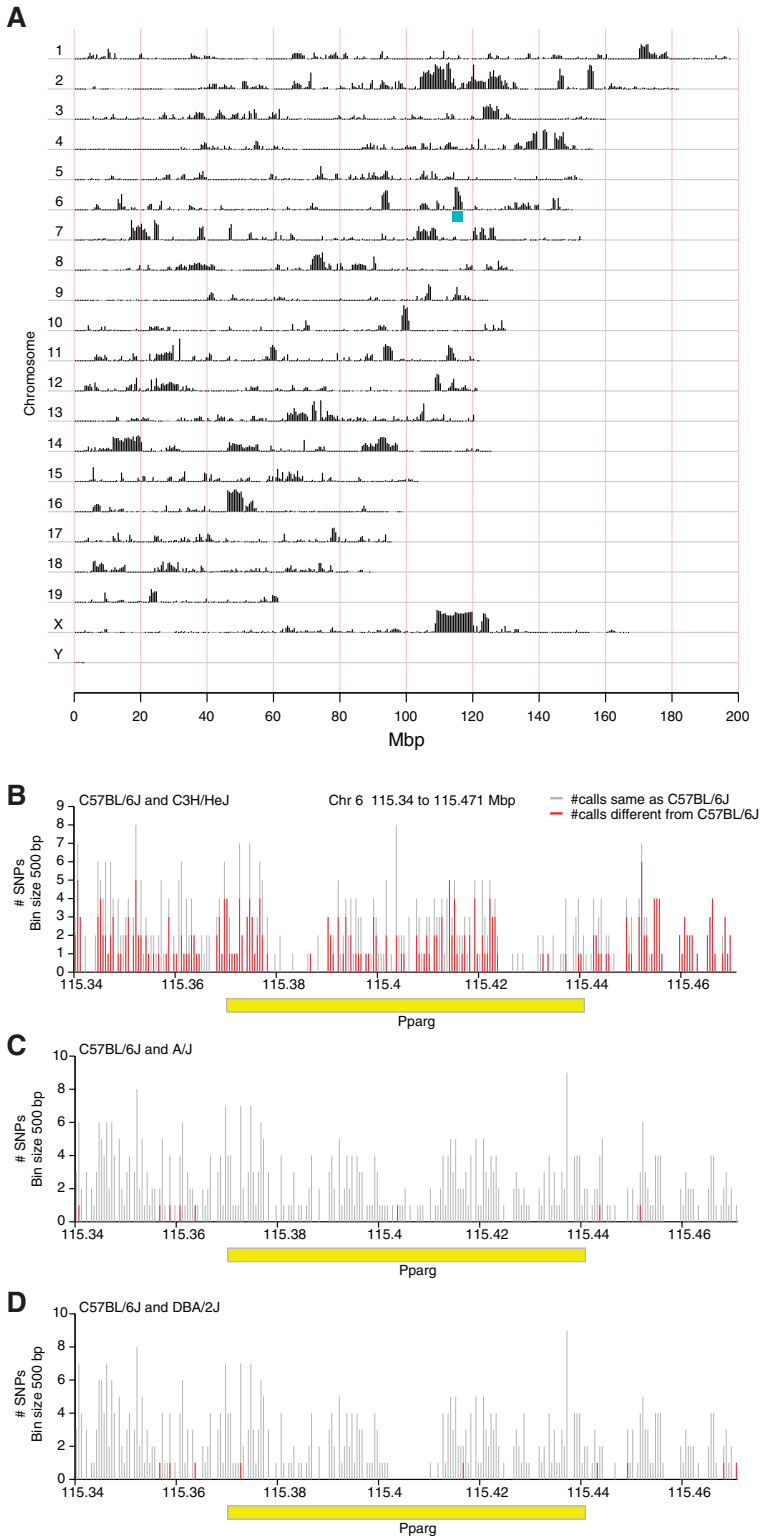

FIG. 5. SNP differences between the inbred strains. A, SNP differences across the entire genome are plotted comparing the C3H/HeJ strain *vs.* the other three strains used in this study: B6, A/J, and DBA/2J. Each chromosome (Chr) is plotted on a separate line. *Vertical black bars* indicate the number of SNPs in that are different between these two strains per 0.5 Mbp window. The genomic location of *Pparg* on Chr 6 is noted in *blue*. B, The region between 115.34 and 115.471 Mbp on Chr 6 (contains the *Pparg* gene) showing the proportion of SNPs having allelic differences when comparing the C3H/HeJ and B6 strains. C, The same region as shown in A displaying allelic differences when comparing B6 with A/J. D, The same region as was shown in A displaying allelic differences when comparing B6 with DBA/2J. The x-axis denotes the genomic location in Mbps and the y-axes the number of SNPs per 500 bp bin. *Vertical red bars* indicate the number SNPs that are polymorphic between the two strains within a given 500-bp bin, and *vertical gray bars* indicate the total number of SNPs for which allele data are available for both strains in a given bin. The *horizontal yellow bar* denotes the *Pparg* gene.

were quite disparate. Osteocalcin is secreted principally by bone cells and has recently been reported to influence insulin secretion and fat metabolism. Moreover, osteocalcin knockout mice have increased visceral fat and serum levels of osteocalcin in humans tends to decline with rosiglitazone treatment (34). Interestingly, in the C3H strain, which showed the most significant decreases in BMD, no changes in serum osteocalcin levels were found. In contrast, for DBA/2J mice, serum osteocalcin levels increased in response to rosiglitazone. Taken together these data suggest that the relationship between circulating osteocalcin and PPARG is likely to be influenced by genetic background and may be more complex than previously considered.

Studies investigating genotype-specific effects of ovariectomy-induced bone loss have suggested that strains with high cortical bone mass are protected from estrogen deficiency-mediated bone loss (35). In this study, the C3H strain, which has the highest cortical vBMD of the four strains studied, exhibited significantly lower cortical vBMD after rosiglitazone treatment. A similar observation was made in the A/J strain, but the A/J strain had much lower cortical vBMD than C3H in the untreated animals. These data suggest that there is little relationship between baseline cortical bone mass and loss of cortical bone with rosiglitazone treatment. Although mice and humans differ in many ways, the inability to predict bone loss based on baseline BMD in our mice would imply that bone mass measurements before treatment with TZDs in humans and would not be particularly helpful in predicting those individuals who will rapidly lose bone on therapy.

We have demonstrated *in vitro*, using a cell culture assay, that activation of PPARG inhibits IGF-I synthesis and secretion (36). However, the results of the present study suggest that the *in vivo* effect of PPARG activation, with regard to IGF-I, is also more complicated than previously recognized. In both the B6 and the C3H strains, an acute drop in serum IGF-I was noted with rosiglitazone, and this decrease was maintained throughout the study. But no differences in serum IGF-I were noted after 1 wk of treatment in the A/J strain, even though a significant decrease was noted at the conclusion of treatment. These results suggest that acute and cumulative responses to rosiglitazone

TABLE 7. KEGG pathways significantly affected by rosiglitazone in C3H and/or B6

KEGG pathway ID	KEGG pathway name	Number of probe sets in pathway	Adjusted Z-score for C3H	Adjusted Z-score for B6
P04110	Cell cycle	279	−6.1	−1.2
P00071	Fatty acid metabolism	99	3.2	2.7
P03320	PPAR signaling pathway	159	5.3	4.8
P00280	Valine, leucine, and isoleucine degradation	89	3.6	2.3
P00240	Pyrimidine metabolism	202	−3.4	−1.2
P04120	Ubiquitin mediated proteolysis	360	−3.5	−0.4
P04115	p53 signaling pathway	187	−3.4	0.3
P00910	Nitrogen metabolism	42	0.8	3.3
P00643	Styrene degradation	3	2.7	3.5

treatment are influenced by independent mechanisms that are subject to allelic variation.

In other studies addressing the effects of rosiglitazone on bone in B6 mice, a consistent decrease in BV/TV% was observed (16, 37, 38). However, there are several key differences between these studies and the present work. In the former studies, male mice of a different substrain of the C57BL/6 strain were used, compared with the C57BL/6JBm strain in our studies. Both Rzonca *et al.* (37) and Lazarenko *et al.* (16) used the C57BL/6, NIA substrain sold by Harlan Sprague Dawley, Inc. (Indianapolis, IN), and Soroceanu *et al.* used a C57BL/6 line supplied by Charles River (Wilmington, MA), which originated from the National Institutes of Health (38). Both of these substrains have been separated from the C57BL/6JBm strain used in these studies for well over 20 generations and can be considered genetically distinct (39). In addition, the studies by Rzonca and Lazarenko used a 20 mg/kg · d dose of rosiglitazone (16, 37), a dose that is approximately 40-fold higher than clinical exposure. In the study by Soroceanu *et al.* (38), the same dose of rosiglitazone was used as was used in this study, but BV/TV% and marrow adiposity were analyzed in a different anatomical location. The differences in gender, substrain, dose, and/or anatomical location studied likely account for the differences between the present study and the previously published observations.

We found site-specific effects on bone mass for both the B6 and DBA/2J strains. This is concordant with human studies by Yaturu *et al.*, who found similar site-specific responses to TZD in diabetic men (19). In the B6 strain, no significant decreases in vBMD or BV/TV% of the femur were found, but a treatment-associated decrease in whole-body aBMD and vertebral vBMD was noted. In the DBA/2J strain, a decrease in vertebral vBMD was found with treatment, but no changes were found for whole body aBMD, femoral BV/TV%, or femoral vBMD. These results emphasize that caution must be exercised when only single BMD measure is used to determined the effects of either a genetic change or a treatment induced change.

It is well established that marrow MSCs can give rise either to osteoblasts or adipocytes, but the relationship between marrow adiposity and trabecular bone volume remains unresolved. There is some evidence suggesting that increases in marrow adiposity are directly associated with decreases in bone mass and volume (40), but in some mouse models, there are also exceptions (41). Evidence to support the first argument comes from both human and animal studies. Observational studies in humans suggest that the volume fraction of the marrow cavity occupied by adipocytes increases with age in both men and women and that this is coincident with a decrease in trabecular bone volume and bone density (9–11, 13). In addition, bone loss is accompanied by increased marrow adiposity in situations of disuse and with treatment by glucocorticoids (41, 42). In rats, ovariectomy results in a decrease in BV/TV% that is associated with increased marrow adiposity (43). A similar effect is observed in older mice treated with rosiglitazone (16, 17). On the other hand, compelling evidence supports the notion that marrow adiposity is not associated with bone volume. Schnitzler and Mequita (44) found, in humans, that it is not the absolute number of adipocytes in the marrow that changes with aging but rather their distribution in the marrow cavity. The early B-cell factor-1 (*Ebf1*) null mouse has substantial increases in marrow adiposity, but this is accompanied by an increase in bone mass and bone formation rate (45). The IRKO-L1, which is a insulin receptor null mouse, in which expression of insulin receptor has been restored in pancreas, liver, and brain, has extremely low numbers of marrow adipocytes but has normal trabecular BMD (46). In this study, we have shown that rosiglitazone can increase marrow adiposity, but this is contingent on the strain examined. Furthermore, changes in marrow adiposity are not necessarily coupled to changes in trabecular bone volume.

Virtually all of the mouse studies published to date have suggested that rosiglitazone has a negative affect on bone, yet all but one of these studies (16, 17, 37, 38), the study by Ali *et al.* (17), examined the effect of rosiglitazone in B6 mice. In this study we have shown that the effect of rosiglitazone on bone in female mice is contingent on the inbred strain studied. These results suggest there is likely a strong gene (or genes) by drug interaction that influences the effect of rosiglitazone on bone in responders *vs.* nonresponders. Genetic differences in the *Pparg* gene alone likely do not account for all the strain-specific responses to this drug nor is every observed drug effect (*i.e.* drop in serum IGF-I or changes in marrow adiposity) likely due to the same genetic differences. Rather our results suggest that the gene by rosiglitazone interaction is polygenic in nature. Interestingly, there are marked allelic differences in the region of the *Pparg* gene when comparing the C3H strain to the other strains, implying that

genetic differences in *Pparg* could partially account for the strong response of this strain to this drug, compared with the other strains.

PPARG has long been known to modulate cell cycle progression (47). In the C3H strain, rosiglitazone treatment was associated with a significant down-regulation of genes associated with cell cycle (Z score = −6.1). In comparison, in the B6 strain, whereas cell cycle gene expression was down-regulated, this result was not significant (Z score = −1.7). This is interesting, given PPARG's known role in the differentiation of MSCs (1, 7, 8); our finding may be the key mechanism by which rosiglitazone negatively impacts on bone. Future studies will examine the effect of PPARG activation on cell cycle progression in the C3H strain.

Genes associated with ubiquitin-mediated proteolysis were found to be significantly down-regulated with treatment in the femur of C3H mice, but this same pathway was not affected in B6. Upon ligand activation, PPARG is quickly degraded via the ubiquitin pathway. In turn, in some forms of cancers, PPARG has been shown alternately to up-regulate or down-regulate the ubiquitin-proteasome system, thus altering levels and activity of other transcriptional regulators (48).

In conclusion, we found a strong interaction between genetic background and the effect of rosiglitazone on body composition, bone mass, and serum IGF-I. These results highlight the importance of considering genetic heterogeneity when interrogating the actions of this class of drugs in mice and humans.

Acknowledgments

The authors thank Drs. Wesley Beamer and Thomas Gridley for their critical review of this manuscript. In addition, the authors thank Mr. Jesse Hammer for his assistance in preparing this manuscript.

Address all correspondence and requests for reprints to: Dr. Clifford J. Rosen, The Jackson Laboratory, 600 Main Street, Bar Harbor, Maine 04609. E-mail: rofe@aol.com.

This work was supported by National Institutes of Health Grants AR45433, AR05460, and AG030910-01.

Disclosure Statement: The authors have nothing to disclose.

References

1. **Spiegelman BM** 1998 PPAR-γ: adipogenic regulator and thiazolidinedione receptor. Diabetes 47:507–514
2. **Krentz A, Bailey C** 2005 Oral antidiabetic agents: current role in type 2 diabetes mellitus. Drugs 65:385–411
3. **Gerstein H, Yusuf S, Bosch J, Pogue J, Sheridan J, Dinccag N, Hanefeld M, Hoogwerf B, Laakso M, Mohan V, Shaw J, Zinman B, Holman R** 2006 Effect of rosiglitazone on the frequency of diabetes in patients with impaired glucose tolerance or impaired fasting glucose: a randomised controlled trial. Lancet 368:1096–1105
4. **Knouff C, Auwerx J** 2004 Peroxisome proliferator-activated receptor-γ calls for activation in moderation: lessons from genetics and pharmacology. Endocr Rev 25:899–918
5. **Rosen E, Sarraf P, Troy AE, Bradwin G, Moore K, Milstone DS, Speigelman BM, Mortensen RM** 1999 PPAR γ is required for the differentiation of adipose tissue *in vivo* and *in vitro*. Mol Cell 4:611–617
6. **Zuo Y, Qiang L, Farmer SR** 2006 Activation of CCAAT/enhancer-binding protein (C/EBP) α expression by C/EBPβ during adipogenesis requires a peroxisome proliferator-activated receptor-γ-associated repression of HDAC1 at the C/ebpα gene promoter. J Biol Chem 281:7960–7967
7. **Lehmann JM, Moore L, Smith-Oliver T, Wilkisin W, Willson T, Kliewer SA** 1995 An antidiabetic thiazolidinedione is a high affinity ligand for peroxisome proliferator-activated receptor γ (PPARγ). J Biol Chem 270:12953–12956
8. **Gimble JM, Robinson CE, Wu X, Kelly K, Rodriguez BR, Kliewer SA, Lehmann JM, Morris DC** 1996 Peroxisome proliferator-activated receptor-γ activation by thiazolidinediones induces adipogenesis in bone marrow stromal cells. Mol Pharmacol 50:1087–1094
9. **Meunier P, Aaron J, Edouard C, Vignon G** 1971 Osteoporosis and the replacement of cell population of the marrow by adipose tissue. A quantitative study of 84 iliac bone biopsies. Clin Orthop Relat Res 80:147–154
10. **Justesen J, Stenderup K, Ebbesen EN, Mosekilde L, Steiniche T, Kassem M** 2001 Adipocyte tissue volume in bone marrow is increased with aging and in patients with osteoporosis. Biogerontology 2:165–171
11. **Verma S, Rajaratnam JH, Denton J, Hoyland JA, Byers RJ** 2002 Adipocyte proportion of bone marrow is inversely related to bone formation in osteoporosis. J Clin Pathol 55:693–698
12. **Shen W, Chen J, Punyanitya M, Shapses S, Heshka S, Heymsfield S** 2007 MRI-measured bone marrow adipose tissue is inversely related to DXA-measured bone mineral in Caucasian women. Osteoporos Int 18:641–647
13. **Griffith J, Yeung D, Antonio G, Lee F, Hong A, Wong S, Lau E, Leung P** 2005 Vertebral bone mineral density, marrow perfusion, and fat content in healthy men and men with osteoporosis: dynamic contrast-enhanced MR imaging and MR spectroscopy. Radiology 263:945–951
14. **Shih T, Chang C, Hsu C, Wei S, Su K, Chung H** 2004 Correlation of bone marrow lipid water content with bone mineral density on the lumbar spine. Spine 29:2844–2850
15. **Nuttall M, Gimble JM** 2000 Is there a therapeutic opportunity to either prevent or treat osteopenic disorders by inhibiting marrow adipogenesis? Bone 27: 177–184
16. **Lazarenko O, Rzonca S, Hogue W, Swain F, Suva L, Lecka-Czernik B** 2007 Rosiglitazone induces decreases in bone mass and strength that are reminiscent of aged bone. Endocrinology 148:2669–2680
17. **Ali A, Weinstein RS, Stewart S, Parfitt AM, Manolagas SC, Jilka R** 2005 Rosiglitazone causes bone loss in mice by suppressing osteoblast differentiation and bone formation. Endocrinology 146:1226–1235
18. **Schwartz A, Sellmeyer D, Vittinghoff E, Palermo L, Lecka-Czernik B, Feingold K, Strotmeyer E, Resnick H, Carbone L, Beamer B, Won Park S, Lane N, Harris T, Cummings S** 2006 Thiazolidinedione (TZD) use and bone loss in older diabetic adults. J Clin Endocrinol Metab 91:3349–3354
19. **Yaturu S, Bryant B, Jain S** 2007 Thiazolidinedione treatment decreases bone mineral density in type 2 diabetic men. Diabetes Care 30:1574–1576
20. **Watanabe S, Takeuchi Y, Fukumoto S, Fujita H, Nakano T, Fujita T** 2003 Decrease in serum leptin by troglitazone is associated with preventing bone loss in type 2 diabetic patients. J Bone Miner Res 21:166–171
21. **Ralston S, de Crombrugghe B** 2006 Genetic regulation of bone mass and susceptibility to osteoporosis. Genes Dev 20:2492–2506
22. **Rosen CJ, Ackert-Bicknell C, Adamo ML, Shultz K, Rubin J, Donahue LR, Horton L, Delahunty KM, Beamer WG, Sipos J, Clemmons D, Nelson T, Bouxsein ML, Horowitz M** 2004 Congenic mice with low serum IGF-I have increased body fat, reduced bone mineral density, and an altered osteoblast differentiation program. Bone 35:1046–1058
23. **Irizarry R, Bolstad B, Collin F, Cope L, Hobbs B, Speed T** 2003 Summaries of Affymetrix GeneChip probe level data. Nucleic Acids Res 31:e15
24. **Cui X, Hwang J, Qiu J, Blades N, GA C** 2005 Improved statistical tests for differential gene expression by shrinking variance components estimates. Biostatistics 6:59–75
25. **Yang H, Churchill GA** 2007 Estimating p-values in small microarray experiments. Bioinformatics 23:38–43
26. **Storey J** 2002 A direct approach to false discovery rates. J R Statist Soc 64: 479–498
27. **Newton M, Quintana F, Den Boon J, Sengupta S, Ahlquist P** 2007 Random-set methods identify distinct aspects of the enrichment signal in gene-set analysis. Ann Appl Stat 1:85–106
28. **Ng A, Wang S, Turner CH, Beamer WG, Grynpas M** 2007 Bone quality and bone strength in BXH recombinant inbred mice. Calcif Tissue Int 81:215–223
29. **Petkov PM, Ding Y, Cassell MA, Zhang W, Wagner G, Sargent EE, Asquith S, Crew V, Johnson KA, Robinson P, Scott VE, Wiles MV** 2004 An efficient SNP system for mouse genome scanning and elucidating strain relationships. Genome Res 14:1806–1811
30. **Beamer WG, Donahue LR, Rosen CJ, Baylink DJ** 1996 Genetic variability in adult bone density among inbred strains of mice. Bone 18:397–403
31. **Beamer WG, Shultz KL, Donahue LR, Churchill G, Sen S, Wergedal JR, Baylink DJ, Rosen CJ** 2001 Quantitative trait loci for femoral and lumbar vertebral bone

mineral density in C57BL/6J and C3H/HeJ inbred strains of mice. J Bone Miner Res 16:1195–1206
32. **Rosen CJ, Ackert-Bicknell C, Beamer WG, Nelson T, Adamo ML, Chohen P, Bouxsein ML, Horowitz M** 2005 Allelic differences in a quantitative trait locus affecting insulin-like growth factor-1 impact skeletal acquisition and body composition. Pediatr Nephrol 20:255–260
33. **Wang L, Shao YY, Ballock RT** 2005 Peroxisome proliferator activated receptor-γ (PPARγ) represses thyroid hormone signaling in growth plate chondrocytes. Bone 37:305–312
34. **Lee NK, Sowa H, Hinoi E, Ferron M, Ahn JD, Confavreux C, Dacquin R, Mee PJ, McKee MD, Jung DY, Zhang Z, Kim JK, Mauvais-Jarvis F, Ducy P, Karsenty G** 2007 Endocrine regulation of energy metabolism by the skeleton. Cell 130:456–469
35. **Bouxsein M, Myers K, Shultz KL, Donahue LR, Rosen CJ, Beamer WG** 2005 Ovariectomy-induced bone loss varies among inbred strains of mice. J Bone Miner Res 20:1085–1092
36. **Lecka-Czernik B, Ackert-Bicknell C, Adamo ML, Marmolejos V, Churchill GA, Shockley K, Reid I, Grey A, Rosen CJ** 2007 Activation of peroxisome proliferator-activated receptor γ (PPARγ) by rosiglitazone suppresses components of the IGF regulatory system *in vitro* and *in vivo*. Endocrinology 148:903–911
37. **Rzonca S, Suva L, Gaddy D, Montague D, Lecka-Czernik B** 2004 Bone is a target for the antidiabetic compound rosiglitazone. Endocrinology 145:401–406
38. **Soroceanu M, Miao D, Bai X, Su H, Goltzman D, Karaplis A** 2004 Rosiglitazone impacts negatively on bone by promoting osteoblast/osteocyte apoptosis. J Endocrinol 183:203–216
39. **Wotjak C** 2003 C57BLack/BOX? The importance of exact mouse strain nomenclature. Trends Genet 19:183–184
40. **Dunnill M, Anderson J, Whitehead R** 1967 Quantitative histological studies on age changes in bone. J Pathol Bacteriol 94:275–291
41. **Lecka-Czernik B, Suva L** 2006 Resolving the two "bony" faces of PPAR-γ. PPAR Res 2006:27489
42. **Motomura G, Yamamoto T, Miyanishi K, Yamashita A, Sueishi K, Iwamoto Y** 2005 Bone marrow fat-cell enlargement in early steroid-induced osteonecrosis—a histomorphometric study of autopsy cases. Pathol Res Pract 200: 807–811
43. **Kurabayashi T, Tomita M, Matsushita A, Honda K, Takakuwa K, Tanaka K** 2001 Effects of a β3 adrenergic receptor agonist on bone and bone marrow adipocytes in the tibia and lumbar spine of the ovariectomized rat. Calcif Tissue Int 68:248–254
44. **Schnitzler C, Mequita J** 1998 Bone marrow composition and bone microarchitecture and turnover in blacks and whites. J Bone Miner Res 13:1300–1307
45. **Horowitz M, Bothwell A, Hesslein D, Pflugh D, Schatz D** 2005 B cells and osteoblast and osteoclast development. Immunol Rev 208:141–153
46. **Irwin R, Lin H, Motyl K, McCabe LR** 2006 Normal bone density in the absence of insulin receptor expression in bone. Endocrinology 147:576–5767
47. **Hsueh WA, Law RE** 2001 PPARγ and atherosclerosis: effects on cell growth and movement. Arterioscler Thromb Vasc Biol 21:1891–1895
48. **Genini D, Carbone G, Catapano C** 2008 Multiple interactions between peroxisome proliferators-activated receptors and the ubiquitin-proteasome system and implications for cancer pathogenesis. PPAR Res 2008:195065